Special Issue

Eletrônica de Potência
Open Journal of Power Electronics

Received July 31, 2024; accepted December 23, 2024; Date of publication January 23, 2025.
The review of this paper was arranged by Associate Editor Qobad Shafiee and Editor-in-Chief Heverton A. Pereira.

Digital Object Identifier http://doi.org/10.18618/REP.e202511

Challenges in Microgrids with Medium Voltage Circuit

Hércules A. Oliveira[1,2,*], **Luiza H. S. Santos**[3], **Luiz A. de S. Ribeiro**[2], **José G. de Matos**[2], **Lucas de P. A. Pinheiro**[1]

[1]Institute of Science and Technology Grupo Equatorial, Research and Development Coordination, São Luís - Maranhão, Brazil.
[2]Federal University of Maranhão, Institute of Electric Energy, São Luís - Maranhão, Brazil.
[3]Universidade Estadual de Campinas, Department of Systems and Energy, Campinas – São Paulo, Brazil.

e-mail: hercules.oliveira@eqtlcontratada.com.br*; l264535@dac.unicamp.br; l.a.desouzaribeiro@ieee.org; gomesdematos@ieee.org; lucas.pinheiro@equatorialenergia.com.br.
* Corresponding author

ABSTRACT This paper presents and discusses challenges in microgrids (μGrid) that arise when they operate isolated from the main grid. Specifically, these challenges occur because the system becomes an ungrounded delta configuration, and the microgrid power sources exhibit low short-circuit capacity. The important issues addressed include the failure to detect ground overcurrent during an earth fault event, voltage imbalances recorded by voltage transformers (VTs) connected between phases and earth, and the phenomenon of ferroresonance. These issues directly impact the coordination of electrical protection, component integrity, and synchronization checks between different power sources within the μGrid. Therefore, the Energy Management System (EMS) is tasked with managing protection devices and systematically responding to minimize disruptions, thereby ensuring operational security. This paper examines the protection functions within devices for both operational modes (on-grid and off-grid) and the corresponding decisions implemented as rules within the EMS. Effective coordination between protection devices and management systems ensures a rapid and selective response to faults, thereby enhancing microgrid security and facilitating efficient problem detection and resolution.

KEYWORDS microgrid, medium voltage, ferroresonance, ungrounded system.

I. INTRODUCTION

The future of electric power systems aims at the deployment of Smart Grids, systems that uses advanced metering and control infrastructure alongside distributed energy resources (DERs) to manage energy [1, 2, 3]. With the data collected in those grids, deploying technologies for predictive maintenance, self-healing, energy efficiency, and grid optimization is possible [4, 5]. Nowadays, distribution systems face technical challenges related to reliability, stability, and security due the growth of DERs applications [6, 7, 8]. In addition, the traditional distribution system was developed without considering DERs, bidirectional power flow, and microgrids connecting and disconnecting from it, creating a whole new set of challenges for their implantation.

As a path towards smart grids, microgrids - a group of interconnected DERs with well-defined electric boundaries that can operate in on-grid (connected) or off-grid (islanded) mode from the utility grid – have been deployed [9, 10]. Using data from DERs, meters, relays and circuit breakers, the energy management system (EMS) of the microgrid makes decisions about its operation and controls of transitions between operation modes. Some of the challenges derived from DERs implementation can be solved or mitigated by proper operation coordination from an EMS in a microgrid [11]. The work in [12] discussed some of those microgrids implantation challenges, such as: i) improper grounding, that could affect the capability of a seamless islanding and grid synchronization, ii) grounding transformer usage to prevent ferroresonance, iii) the absence of studies discussing relay settings and how important it is to keep the voltage and frequency values within specified range even during transitions, and iv) how delays in communication – especially with the relay at the point of common coupling (PCC) – can affect the implementation of transition algorithms. All those challenges were discussed and overcome in a medium voltage microgrid in the electrical distribution system of the United States, by properly connecting and disconnecting the grounding transformer and coordinating the protection. However, each microgrid has its own challenges, once they are uniquely sized and deployed, depending on the region, electric grid, and combination of DERs. Therefore, implementing μGrids requires customized technical solutions for feasibility.

Most of the challenges faced during the microgrid deployment are the combination of technical issues already faced before, such as ferroresonance [13], short-circuit level, absence of inertia on inverter-based DERs [14]. As those deployments comprise multidisciplinary knowledge (EMS, power electronics, protection parametrization, telecommunications, data management), it takes those issues to another level by creating correlations among them. As for implementation, microgrids are highly indicated for critical facilities, such as hospitals, data centers, and military installations, once they can improve reliability, energy independence, enhanced resilience, and energy efficiency [15, 16]. To further discuss those challenges, the microgrid at the Alcântara Launch Center (ALC-µGrid) [17], shown in

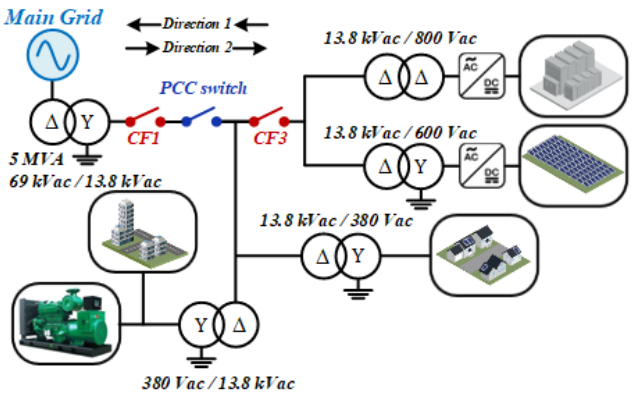

FIGURE 1. Simplified diagram of the ALC-µGrid medium voltage network [17].

FIGURE 1, is a real system and will be used as a case study in this paper.

The ALC-μGrid aims for high resilience and operational security, especially during the rocket launch campaigns, because it comprises critical installations and assets which require power supply with high energy quality (e.g., rocket trajectory tracking). Without the microgrid, the facility depends on the local utility grid, subject to interruptions that could ruin the launch campaign, leading to financial losses and security issues [18].

This paper presents the challenges regarding protection, parameterization of protection relays, and ferroresonance, while developing the ALC-μGrid and the appropriate technical solutions to solve them, as an extended version to what was presented in [17]. Once microgrids are customized systems, the challenges description and the technical solutions adopted may contribute to microgrids in development to reach an automatic and safe operation. The main contributions are: 1) understanding the causes of ferroresonance in an isolated microgrid, and how to mitigate them; 2) coordination protection design between the PCC switch and the converter of the Battery Energy Storage System (BESS) to guarantee a seamless transition to off-grid mode during power quality problems in the main grid, and presentation of operational results of a real life microgrid.

II. DESCRIPTION OF THE SYSTEM AND CHALLENGES

The ALC-μGrid, is connected to a medium voltage (MV) utility substation through a Δ-Y transformer with solidly grounded neutral, and can be disconnected from the main grid using a switch at the PCC, as shown in FIGURE 1. The microgrid is composed of a 1.25 MWp of solar panel, 1.125 MVA of Diesel Generator Set (DGS), 1 MW/1MWh of BESS, critical and non-critical loads.

In a conventional system, current, voltage, and frequency protections must be implemented with the criterion of preserving the integrity of the equipment and components of the electrical system, substations, loads, and generation sources. However, the presence of distributed generation adds to this issue the possibility of reverse current flow, even in a radial grid, and the supply of potential short-circuits by more than one source at electrical nodes located at different points in the distribution grid. Additionally, microgrids have some particularities such as:

- Even though remotely controlled switches are supervised by the EMS, they operate individually, with coordination defined based on the parameterization of protection devices, for example, multifunction relays;
- In the event of a switch opening due to the operation of the respective overcurrent protection, reclosing will only be possible after the execution of an inspection protocol and clearance from the operation and maintenance team.

In this context, due to the contributions of distributed sources, microgrids must have protection profiles according to the mode of operation (on-grid and off-grid) and the direction of power flow.

When the PCC switch is opened, the microgrid operates in an off-grid mode, becoming an ungrounded electrical system. This configuration presents several challenges, including the inability to detect earth overcurrent in case of a single-phase earth fault event, voltage imbalance between phase-to-earth measurements using the VTs, and ferroresonance.

According to [13], ferroresonance is a nonlinear phenomenon that arises due to resonance of capacitive circuits and nonlinear inductors in transformers (power and VTs) under specific conditions, leading to overvoltage and overcurrent that can damage insulation and components.

The ALC-μGrid experiences ferroresonance due to various factors, including the presence of parasitic capacitances in ungrounded distribution lines, magnetization inductances of VTs, low load conditions, and the ungrounded nature of the MV system when in off-grid mode. This phenomenon has been observed during black start conditions (FIGURE 2), even with the voltage ramp that is controlled by the converter of the BESS.

III. IMPLEMENTED SOLUTIONS AND DISCUSSION OF RESULTS

This section shows the solutions to four main problems faced during ALC-μGrid development: a) measurement problems, b) ferroresonance, c) voltage and frequency protection, and d) current protection.

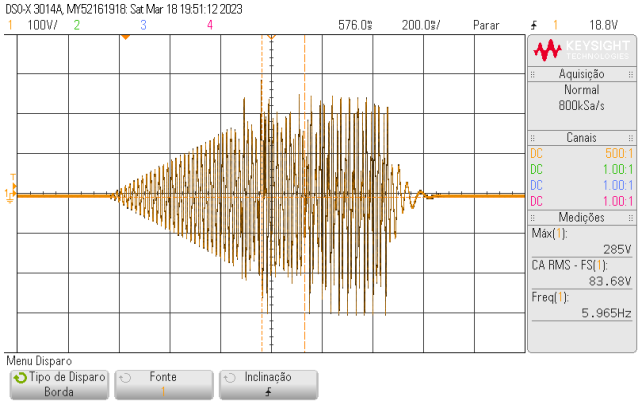

FIGURE 2. Phase-to-earth voltage in the at black start with voltage ramp (ferroresonance).

A. *MEASUREMENT PROBLEMS*

The measurement and protection systems with three VTs in Y connected between phases-to-earth in the MV side of the circuit breakers of ALC-μGrid form a load in Y with the common point without connection to the source (isolated neutral). Suppose each phase equivalent impedances are not equal, due to phase-to-earth parasitic capacitances and the magnetizing impedances of the respective VTs. In that case, they form a Y-unbalanced load with neutral displacement. This results in different voltage measurements even though the real voltages are balanced. In the case of systems that use four VTs, three at the input of the MV circuit breaker and one at the output (used for bus voltage and synchronism checks), there will be an imbalance between the equivalent impedances between each phase and the grounded common point. In this case, there will be a neutral shift, and voltage measurement errors can be greater.

Voltages were measured on the secondary side of VTs of the BESS MV circuit breaker during a transition from on-grid to off-grid mode. It can be seen in FIGURE 3 that the phase-to-earth voltages became unbalanced after the PCC switch is opened and the system starts to operate in off-grid mode. However, line voltages do not present noticeable distortion or imbalance in this context (FIGURE 4).

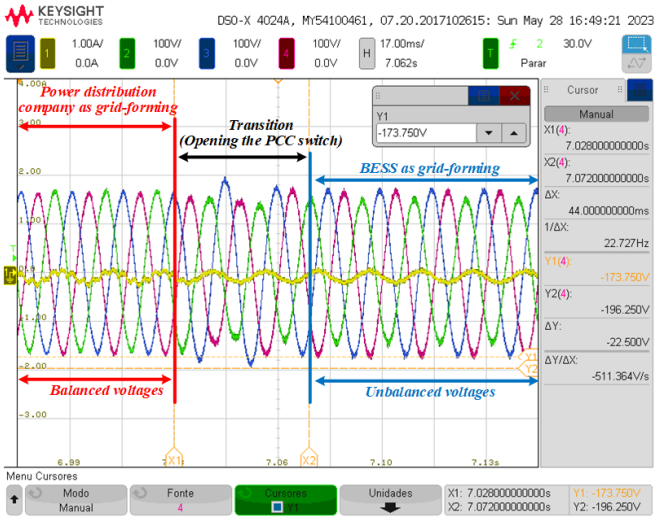

FIGURE 3. Phase-to-earth voltages measured on the secondary of the BESS MV circuit breaker VTs.

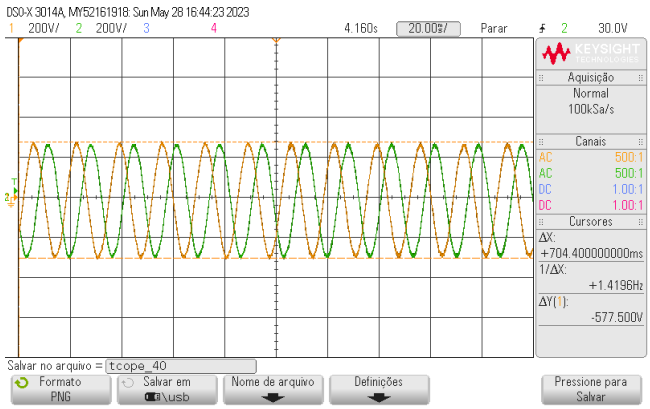

FIGURE 4. Line voltages measured on the secondary of the BESS MV circuit breaker VTs.

An alternative solution for the synchronism check when having voltages from different sources on both sides of the MV circuit breaker is to connect the synchronism check VT between phases, since it is possible to adjust the voltage amplitude and angle in the settings of the protection relay for equivalence with the phase-to-earth voltage of the synchronism check.

B. *FERRORESONANCE*

In the distribution grid, lines have phase-to-earth capacitances and inductive VTs connected between phase-to-earth have low excitation current and high non-linear magnetizing inductance. If the inductive reactance of the VTs is equal to or close to the parasitic capacitive reactance of the system, the set may form a poorly damped resonant circuit, which may result in ferroresonance.

These grids consist of numerous saturable inductances and capacitors, including power transformers, inductive and capacitive voltage measuring transformers, shunt reactors, series or shunt capacitor banks, cables, and long transmission lines. As a result, these elements create conditions conducive to the occurrence of ferroresonance scenarios.

FIGURE 5 shows a basic series ferroresonance circuit, from which the phenomenon of ferroresonance can be discussed in a simplified way, further details are discussed in [13]. In the initial condition, once the source is switched on ($t = t_0$), voltage at the capacitance terminals is assumed equal to V_{C0} and a current I is created and oscillates at frequency $\omega_1 = 1/\sqrt{LC}$, where L and C represent the coil inductance and capacitance, respectively. The flux in the coil and the voltage V_{c1} across the capacitor terminals are then expressed as (1) and (2).

$$\phi = \frac{V_{c0} \sin \omega_1 t}{\omega_1} \tag{1}$$

$$V_{c1} = V_{c0} \cos \omega_1 t \tag{2}$$

If $V_{c0}/\omega_1 > \phi_{sat}$, the flux ϕ reaches the saturation flux ϕ_{sat}, voltage V_{c1} is equal to V_1 and the inductance of the saturated coil becomes L_s ($t = t_1$). As L_s is very small compared to its initial value L, the capacitor suddenly "discharges" across the coil in the form of an oscillation of frequency $\omega_2 = 1/\sqrt{L_s C}$. The current and flux peak when the electromagnetic energy stored in the coil is equivalent to the electrostatic energy $1/2CV_1^2$ stored by the capacitor. When the flux returns to ϕ_{sat} ($t = t_2$), the inductance reassumes the value L and, since the losses have been ignored, voltage V_{c1}, which has been reversed, is equal to $-V_1$. When the flux reaches $-\phi_{sat}$ the voltage V_{c1} is equal to $-V_2$ ($t = t_3$). As ω_1 is in practice very small we can consider $V_2 \cong V_1 \cong V_{c0}$. As a result, the oscillation period (T) in the non-saturated condition is included between $2\pi\sqrt{LC}$, and in

saturation condition is $2\pi\sqrt{L_sC} + 2(t_3 - t_2)$. Consequently, the corresponding frequency is represented by (3) and (4).

$$f = \frac{1}{T} \tag{3}$$

$$\frac{1}{2\pi\sqrt{LC}} < f < \frac{1}{2\pi\sqrt{L_sC}} \tag{4}$$

The initial frequency depends on some variables such as the saturation flux, non-linearity of electrical components and initial voltage at the capacitance terminals. As a result, the voltage waveform can be affected in different ways by the ferroresonance effect, as shown in FIGURE 6. A real waveform with the effect of ferroresonance in a single-phase of the circuit is shown in FIGURE 7. This oscilloscope measurement recording was made from the case study microgrid before a solution to this problem was implemented.

Among the various solutions proposed in the literature to mitigate this phenomenon, it was decided to use damping resistors on the secondary side of the VTs, which must be sized to not exceed the rated load of the VTs [13]. This was the solution chosen because it is cheaper than others indicated in the literature and because it provides satisfactory results. Once the VTs windings were connected as shown in FIGURE 8 (in Y-Y), the damping resistor was dimensioned using the equation (5).

$$R = \frac{U_S^2}{k \times P_t - P_m} \tag{5}$$

Where R is the damping resistance value in Ohms, U_S is the rated secondary voltage of the VT, k factor between 0.25 and 1 such that errors and service conditions remain within the limits specified by standard IEC 186 [19], P_t is the rated output power of the VT, and P_m is the power required for measurement.

The ALC-μGrid VTs are $(13.8\,\text{kV}\sqrt{3})\ /115\,\text{V}$, class 0,3P75. The maximum power the TP can feed without compromising its accuracy class of 0.3 % is $P_t = 75\,\text{kW}$. Each voltage input from PEXTRON URP 6000 relay, which was the model used in ALC-μGrid, has a load equal to $P_m = 0.14\,\text{W}$. Substituting those values in (5) and arbitrating k as 0.8, R is defined in (6).

$$R = \frac{115^2}{(0.8 \times 75) - 0.14} \rightarrow R = 220.93\,\Omega \tag{6}$$

To check the power dissipation P_R of the damping resistor, the calculation goes as follows in (7).

$$P_R = \frac{U_S^2}{R} = \frac{115^2}{220{,}93} = 59.86\,\text{W} \tag{7}$$

A thermography made of the damping resistor mounted on a heatsink on the secondary side of the VT in one of the MV circuit breakers at ALC-μGrid is shown in FIGURE 9. The concern is to ensure that the nominal working temperature does not reduce the power dissipation capacity of the

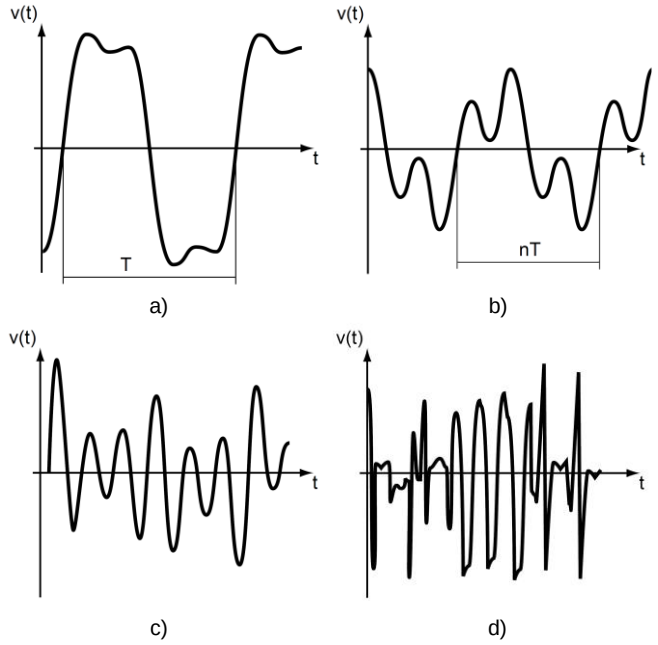

FIGURE 6. Illustration of ferroresonance characteristics [13]: a) fundamental mode, b) subharmonic mode, quasi-periodic mode, and d) chaotic mode.

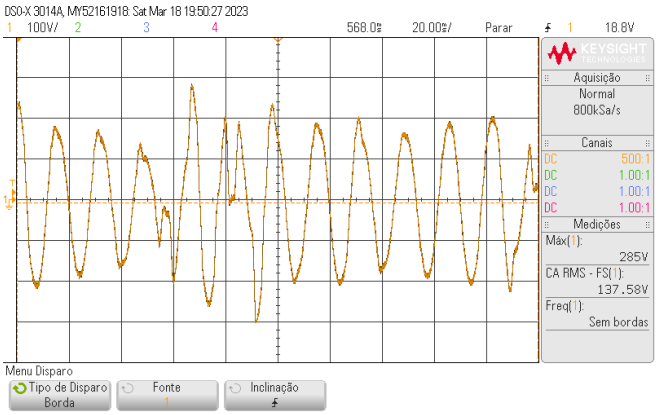

FIGURE 7. Ferroresonance effect in single-phase circuit.

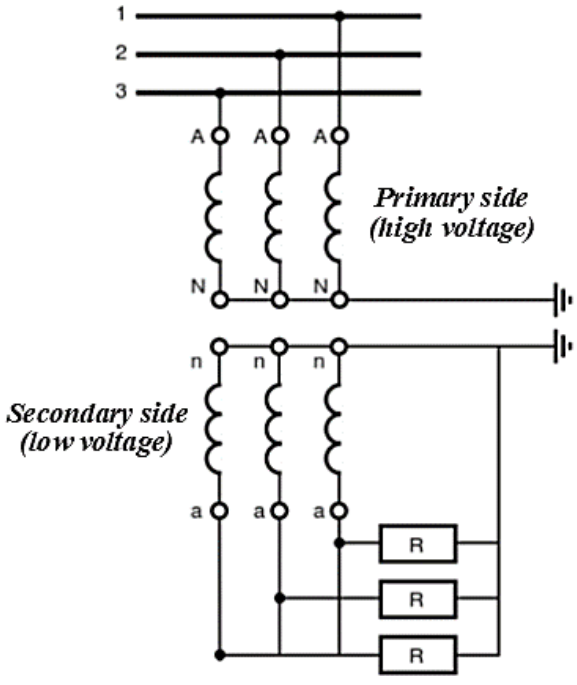

FIGURE 8. Connection form of VTs in ALC-μGrid [13].

damping resistor. The model (AP101 100W TO-247) used has an operating temperature range from −65°C up to +175°C [20]. Since the maximum temperature recorded was 114 °C, the resistor operates under normal conditions.

After the solution with the damping resistors had been installed, the black start conditions were tested again. As shown in FIGURE 10 when comparing with FIGURE 2, the ferroresonance was solved, since the phase-to-earth voltages do not resonate and are in acceptable range. Based on the results presented, it was possible to avoid overvoltage protections and to guarantee the integrity of the components.

C. *VOLTAGE AND FREQUENCY PROTECTION*

In the study and coordination of protection, the main considerations for voltage protections were:

i. To be slower than current functions to maintain energy continuity and avoid unwanted trips due to intermittent voltage variations caused by distributed generation;

ii. The sequence of priority for the operation of switches and sources in the event of under or overvoltage events follows this order: first, the PCC switch; next, the intrinsic ones to the BESS; and then the medium voltage circuit breakers of the internal substations. In this way, in some cases, it is possible to manage the system to isolate faults and continue supplying energy;

iii. The closing of the switches after operating due to voltage function is done automatically after timed reclosures of the protection relays. This time is sufficient for the voltages to return and remain stable, thereby avoiding unnecessary or unwanted successive trips.

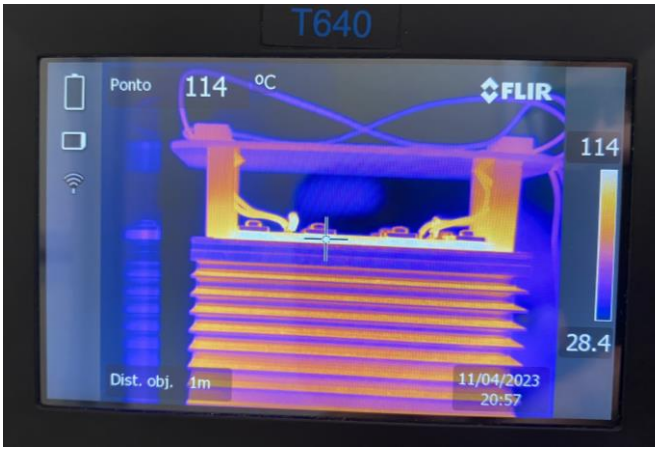

FIGURE 9. Thermography of the resistor and heatsink installed on the secondary of the VTs.

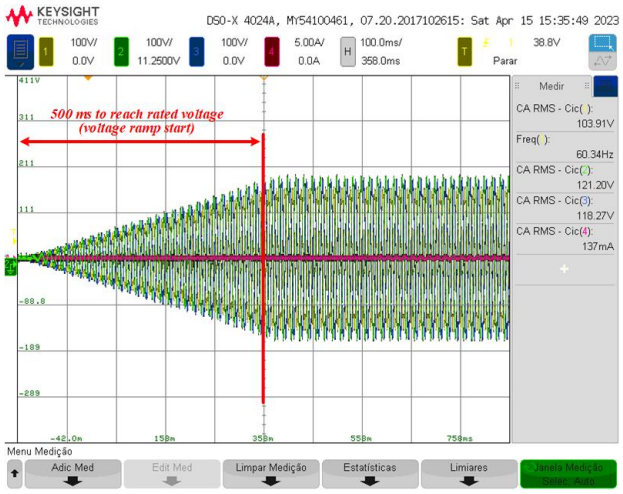

FIGURE 10. Phase-to-earth voltages at black start with damping resistor.

The voltage and frequency protections on the PCC switch were defined with the aim of the switch operating before the protections set on the Power Converter System (PCS), ensuring power supply to loads. The values set on the PCC switch took into account the local power utility company standards and field surveys on the values and frequency of occurrence for voltage sags and swells at the point of connection to the main grid. Voltage sags can be of low amplitude and momentary due to load and generation dynamics, or they can be of large amplitude due to critical events in the grid.

The parametrization of protection relays is simpler when it is possible to set multiple voltage setpoints based on the amplitude and trip time. However, not all relays offer the flexibility to configure multiple setpoints for undervoltage and overvoltage protection. An alternative solution to this limitation is to use positive, negative, and zero sequence voltage protections.

The PCC switch was parameterized considering these protections, as presented in TABLE 1, to operate according to the graph shown in FIGURE 11.

The voltage protection was configured as follows:

- Minor voltage sags are tolerated for a longer duration since the BESS consistently provides voltage support to the main grid;
- Significant voltage sags are tolerated for a shorter duration due to the BESS's rapid capability to switch from grid-following to grid-forming mode.

TABLE 1. PCC switch protection setpoints.

Positive Sequence	
Open-Source Voltage Threshold	80 %
Open-Source Time to Trip	0.1 s
Single-Phasing Protection and Sectionalizing	
Zero sequence voltage Threshold	30 %
Zero sequence current restraint Threshold	10 A
Negative Sequence Voltage Threshold	10 %
Negative Sequence Current Restraint Threshold	100 A
Unbalance Time to Trip (s)	0.1 s
Trip on Single-Phase Voltage	
Single-Phase Low Voltage Threshold	80 %
Single-Phase High Voltage Threshold	110 %
Single-Phase Low Voltage Time to Trip	1 s
Single-Phase High Voltage Time to Trip	0.2 s
Trip on Three-Phase Voltage	
Three-Phase Low Voltage Threshold	80 %
Three-Phase High Voltage Threshold	110 %
Three-Phase Time to Trip	0.1 s

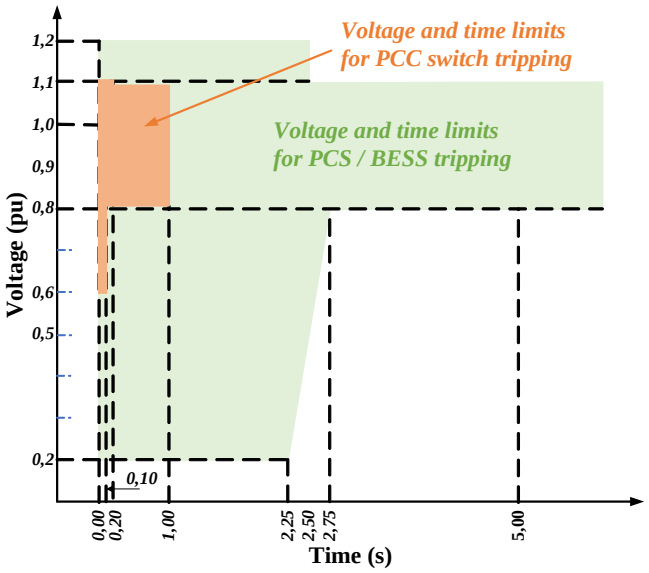

FIGURE 11. Voltage and time limits for PCC switch and PCS/BESS tripping.

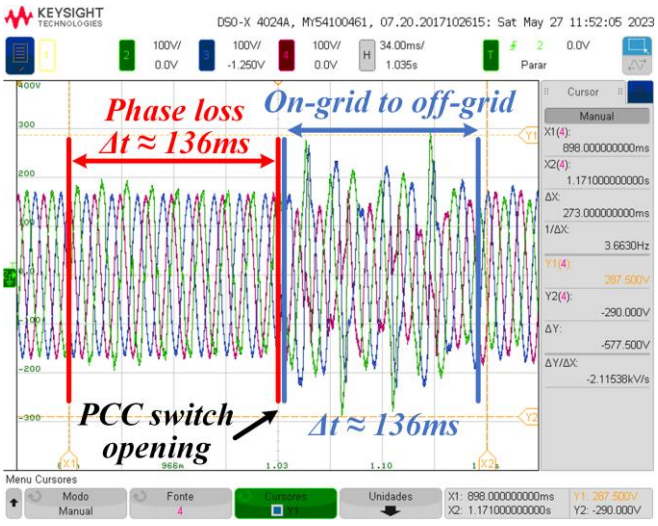

FIGURE 12. Voltage protection actuation on the PCC switch after phase loss.

In on-grid mode, the microgrid has an anti-islanding function, where an event in the main grid triggers a trip at the PCC switch, and the BESS takes over the internal grid as presented in FIGURE 12. A test was carried out on the microgrid in which one grid phase was opened before the PCC switch and the protection acted according to the settings. The PCC switch took 136 ms to open after a phase loss and the BESS was able to maintain the lost phase voltage on the microgrid side. After opening the PCC switch, voltage transients were less than 136 ms and it did not activate the voltage protections. In this test, initially the BESS operated in grid-following mode without absorbing or injecting power into the main grid and the photovoltaic plant was injecting 612 kW. Considering the load during the test, the excess power was approximately 375 kW, which was exported to the main grid through the PCC switch.

In off-grid mode, with the BESS as a grid-forming and the DGS operating as grid-following, the DGS take over the grid in the event of a BESS failure.

Whenever the ALC-μGrid is operating in off-grid mode, the converter of the BESS feeds the medium voltage distribution line through a $\Delta - \Delta$ transformer. A single-phase earth fault does not activate the earth overcurrent protection in a distribution grid whose transformers are in ungrounded delta (medium voltage side), such as the topology of the ALC-μGrid. An alternative solution for a single-phase earth fault detection is to use three VTs connected in Y with the common point grounded and configure the neutral overvoltage function in the protection relay, using the neutral residual voltage (3V0) to activate the protection. The 3V0 voltage in a single-phase earth fault event is theoretically 300 % of the rated phase-to-earth voltage of the system. Therefore, a lower setting (for example, 225 %) can be used to detect the fault. The VTs and surge arresters of the phases without earth fault are subjected to a line voltage. Therefore, quickly detecting the fault can prevent components such as VTs and surge arresters from being damaged. The supplier datasheets usually report these components' peak voltage withstand and transient duration.

In the case of the ALC-μGrid, a smaller adjustment than the withstand time of the distribution surge arresters (300 ms) for transition overvoltages (TOV) was used, as it is smaller than the withstand time of the VT. This solution proved to be effective in an earth fault event, in which there was a contribution from microgrid sources. However, the waveforms are not shown in this paper because this was a real and random event.

It is important to have protection for detecting the opening of a phase in the MV grid, which is critical in:

i. Either on-grid or off-grid mode: the opening of a phase on the MV grid side and at the BESS output, because the voltages produced by the PCS can render ineffective the undervoltage protections of the MV relay at the BESS substation. This is because the MV circuit breaker will be closed and with voltages on all three poles, considering that the phase opening is in the circuit external to the substation. In this case, it is necessary to provide protection that isolates the source (BESS);
ii. Off-grid mode: the opening of a phase on the MV grid side at the DGS substation output, with them operating in grid-following mode with the BESS or grid-forming, as the voltages produced by the DGS can render ineffective the undervoltage protections of the relay. This is analogous to the previous item. In this case, it is necessary to provide protection that isolates the source (DGS);
iii. On-grid mode: the opening of a phase on the upstream side of the PCC switch, as the voltages produced by the BESS can render ineffective undervoltage protections of the relay at the PCC switch.

The solution for the conditions of the scenarios described was to implement the protection function sensitive to the negative sequence current component (ANSI 46 BC function) [21]. This allows the identification of the open phase conductor in the MV grid (broken conductor or open fuse switch), especially when this cannot activate the undervoltage or negative sequence voltage protections [21].

Regarding the synchronization check protection, ANSI 25 function [21], the closure of the PCC switch with both sides

energized can only be done if the voltages on the microgrid side and the utility grid side are synchronized with each other and within acceptable tolerances. If the ANSI 25 function [21] is not being met, the PCC switch is blocked and does not execute the closing command, even if this command is sent by the EMS. The tolerance adjustments for the differences in frequency, amplitude, and phase angle of the voltages on both sides of the switch were determined based on computer simulations of the switch closure, technical standards of the local energy utility, and tests during commissioning [22]. The values implemented in the switch are as follows:

- Voltage difference limit 13 %;
- Phase angle difference limit 5°;
- Frequency difference limit 0.2 Hz;
- Voltage limit above which the synchronization check is performed 20 %;
- Synchronization verification wait time 300 s.

The values were defined based on the accuracy of the voltage, frequency, and angle measurement devices used, and to prevent current transients during the switch closure that could activate the PCS overcurrent protection.

D. *CURRENT PROTECTION*

The current protection in the microgrid has some particularities such as:

i. The contribution of the sources to a short-circuit considering the direction of power flow, one from the microgrid to the utility grid (Direction 1), and the other from the utility grid to the microgrid (Direction 2), as shown in FIGURE 1.

ii. The parameterization of protection devices based on coordination that allows for the isolation of faults and the operation of part of the microgrid, with grid-forming systems, as long as it is done safely.

iii. The management of medium and low voltage circuit breakers and reclosers after fault events to readjust microgrid topology, ensuring power supply to all possible loads. However, in short-circuit situations, the remote closing of these circuit breakers must follow an inspection, maintenance, and operation protocol.

Following the defined power flow for each direction, the adjustments considered for Direction 2 must protect the system from short-circuits within the microgrid, stopping the utility grid's contribution to these fault currents. For this type of fault, the PCC relay only responds to the utility grid contribution with both timed and instantaneous current functions, for phase and neutral.

The current protection settings of the PCC relay must be coordinated with the utility grid substation relay in the power utility feeder. These protections must also have a sufficient range so that the microgrid's internal MV relays (downstream to the PCC switch) adjustments are coordinated with the PCC relay and fuse switches (FIGURE 1).

The pick-up value for the timed current phase function was set at 150% of the maximum load current at the PCC in steady state, which is below the permissible current for the conductor in the MV lines (in the case study). Additionally, the settings for both timed and instantaneous phase functions should not be activated by the total inrush current from the transformers upstream of the PCC switch. For ground faults, the pick-up

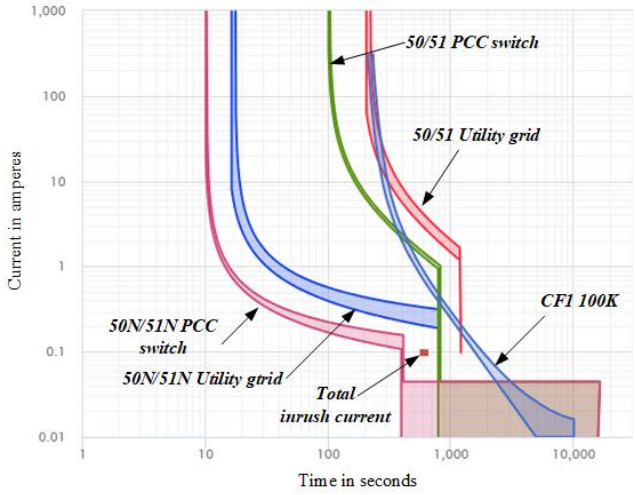

FIGURE 13. Current curve for coordination in direction 2.

current setting for the timed current neutral function should be between 10% and 45% of the maximum load current in steady state [23]. The time-current curves for the utility grid feeder relay, PCC switch, and CF1 100 K fuse switch are shown in FIGURE 13.

The adjustments for Direction 1 must prevent internal sources of the microgrid from contributing to short-circuits and limit the power injected by the microgrid into the utility grid in the event of EMS power control failure. Since the BESS and the solar panel plant operate as grid-following in on-grid mode, their short-circuit contribution between phase currents must be limited to their rated power.

Because the internal sources are connected to the utility grid through isolated coupling transformers with the medium voltage side in delta, they do not contribute to earth faults on the utility grid side. Therefore, both timed and instantaneous neutral functions in Direction 1 can be disabled. The time-current curves for the BESS, solar panel plant, PCC switch, and CF3 65 K fuse switch are shown in FIGURE 14.

As shown in FIGURE 14, the current curves are spaced by the actuation time, making it possible for the microgrid to continue supplying loads or parts of them in some events of trip. The protection devices are activated in the following sequence: both timed and instantaneous neutral functions of the BESS and solar panel plant; both timed and instantaneous

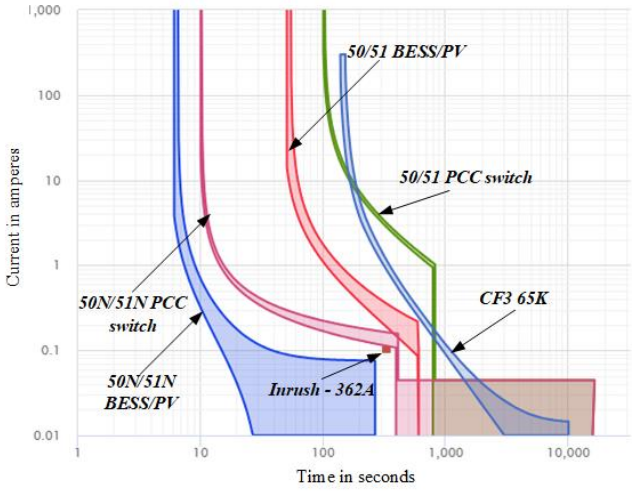

FIGURE 14. Current curve for coordination in direction 1.

neutral functions of the PCC switch; both timed and instantaneous phase functions of the BESS and solar panel plant; and both timed and instantaneous phase functions of the PCC switch. The trip of the fuse switch depends on the fuse link capacity, which in this case will act between the timed and instantaneous phase function curves of the BESS, solar panel plant, and the PCC switch.

IV. CONCLUSION

This article discussed the challenges in microgrids, focusing on operating isolated from the main grid and with ungrounded medium voltage circuits. Several approaches were taken regarding specific solutions applied to individual components, the parameterization of protection components, the coordination of their settings, and the energy management system that controls the microgrid.

The solutions presented to mitigate the problems of the ferroresonance phenomenon have shown technically satisfactory results. Using resistive loads in the VTs secondaries minimize the overvoltages and voltage distortions in the phase-to-earth voltage waveforms. Furthermore, the proposed parameterization of the relay allowed for synchronism checks between two different sources and the detection of single-phase earth faults. This avoids having a system with 4 VTs connected in Y-Y with 2 of them connected to the same phase, which would form an unbalanced Y load, and consequently unbalanced voltage measurements could be indicated by the measuring VTs.

The parameterization of the protection devices was developed considering two approaches regarding short-circuit contributions, from the microgrid to the utility grid and from the utility grid to the microgrid.

Additionally, voltage and frequency protections were implemented to detect faults missed by the current protection functions such as short-circuits, phase-to-ground faults with the microgrid operating in off-grid mode (ungrounded system), and islanding detection.

From all these approaches, it was possible to develop and implement a set of relay parameterization, the coordination of protection devices, and a protection management system with improved performance, ensuring the safety of components, loads, and systems. This also improved the continuity of power supply through the reconfiguration of the microgrid in the event of contingencies.

ACKNOWLEDGMENT

This work was supported by the Institute of Science and Technology Grupo Equatorial and Grupo Equatorial through the PDI ANEEL program under grant PD-06072-0702/2023. This work was also supported by São Paulo Research Foundation - FAPESP (Grant: 2022/03441-7, and thematic project 2021/11380-5), by the Coordenação de Aperfeiçoamento de Pessoal de Nível Superior – Brasil (CAPES), and Conselho Nacional de Desenvolvimento Cientifico e Tecnológico – Brasil (CNPq).

AUTHOR'S CONTRIBUTIONS

H. A. OLIVEIRA: Conceptualization, Data Curation, Formal Analysis, Investigation, Methodology, Project Administration, Software, Supervision, Validation, Visualization, Writing – Original Draft, Writing – Review & Editing. **L. H. S. SANTOS:** Conceptualization, Data Curation, Formal Analysis, Investigation, Software, Visualization, Writing – Review & Editing. **L. A. S. RIBEIRO:** Conceptualization, Data Curation, Formal Analysis, Investigation, Methodology, Project Administration, Resources, Software, Supervision, Validation, Visualization. **J. G.MATOS**: Conceptualization, Data Curation, Formal Analysis, Investigation, Methodology, Software, Validation, Visualization. **L. P. A. PINHEIRO**: Funding Acquisition, Project Administration, Resources, Supervision, Visualization.

PLAGIARISM POLICY

This article was submitted to the similarity system provided by Crossref and powered by iThenticate – Similarity Check.

REFERENCES

[1] H. Farhangi, "The path of the smart grid," *IEEE power and energy magazine*, vol. 8, pp. 18-28, 2009, doi: 10.1109/MPE.2009.934876

[2] A. Muhtadi, D. Pandit, N. Nguyen and J. Mitra, "Distributed energy resources based microgrid: Review of architecture, control, and reliability," *IEEE Transactions on Industry Applications*, pp. 2223-2235, 2021, doi: 10.1109/TIA.2021.3065329

[3] K. dos Santos, L. Santos, N. Bañol, J. C. López, M. J. Rider and L. C. d. and Silva, "Optimal Sizing and Allocation of Distributed Energy Resources in Microgrids Considering Internal Network Reinforcements," *Journal of Control, Automation and Electrical Systems*, pp. 106-119, 2023, doi: 10.1007/s40313-022-00934-x

[4] S. Ahmad, M. Shafiullah, C. B. Ahmed and M. Alowaifeer, "A Review of Microgrid Energy Management and Control Strategies," *IEEE Access*, 2023, doi: 10.1109/ACCESS.2023.3248511

[5] Y. Wu, J. M. Guerrero, Y. Wu, N. Bazmohammadi, J. C. Vasquez, A. J. Cabrera and N. Lu, "Digital Twins for Microgrids: Opening a New Dimension in the Power System," *IEEE Power and Energy Magazine*, vol. 22, pp. 35--42, 2024, doi: 10.1109/MPE.2023.3324296

[6] H. A. Oliveira, J. G. De Matos, L. A. d. S. Ribeiro, O. R. Saavedra, A. d. A. Lorençato, A. S. Martins and L. d. P. A. Pinheiro, "Smooth Integration of Rectifier-Battery Banks Operation in Real-Life Isolated Microgrids Based on Renewable Sources: Theory and Application," *IEEE TRANSACTIONS ON SMART GRID*, pp. 3383-3393, 5 September 2022, doi: 10.1109/TSG.2022.3171447

[7] S. Tan, Y. Wu, P. Xie, J. M. Guerrero, J. C. Vasquez and A. Abusorrah, "New Challenges in the Design of Microgrid Systems: Communication Networks, Cyberattacks, and Resilience," *IEEE Electrification Magazine*, pp. 98-106, 2020, doi: 10.1109/MELE.2020.3026496

[8] R. O. d. Sousa, A. F. Cupertino, L. M. F. Morais, H. A. Pereira and R. Teodorescu, "'Experimental Validation and Reliability Analyses of Minimum Voltage Control in Modular Multilevel Converter-Based STATCOM," *IEEE Transactions on Industrial Electronics*, pp. 1-10, 2023, doi: 10.1109/TIE.2023.3303634

[9] D. T. Ton and M. A. Smith, "The US department of energy's microgrid initiative," *The Electricity Journal*, vol. 25, pp. 84-94, 2012, doi: 10.1016/j.tej.2012.09.013

[10] N. Hatziargyriou, Microgrids: architectures and control, John Wiley & Sons, 2014.

[11] J. D. L. Cruz, Y. Wu, J. E. Candelo-Becerra, J. C. Vásquez and J. M. Guerrero., "A review of networked microgrid protection: Architectures, challenges, solutions, and future trends," *CSEE Journal of Power and Energy Systems*, 2023, doi: 10.17775/CSEEJPES.2022.07980

[12] S. L. Aleksandar Vukojevic, "Microgrid protection and control schemes for seamless transition to island and grid synchronization," *IEEE Transactions on Smart Grid*, vol. 11, pp. 2845--2855, 2020, doi: 10.1109/TSG.2020.2975850

[13] P. Ferracci, "Ferroresonance," in *Collection Technique*, Groupe Schneider, 1998, pp. 1-30.

[14] P. Singh, U. Kumar, N. K. Choudhary and N. Singh, "Advancements in Protection Coordination of Microgrids: a Comprehensive Review of Protection Challenges and Mitigation Schemes for Grid Stability," *Protection and Control of Modern Power Systems*, vol. 9, pp. 156-183.

[15] C.-N. a. L. J. J. a. C. Y.-C. Huang, "A method for exploring the interdependencies and importance of critical infrastructures," *Knowledge-Based Systems*, vol. 55, pp. 66-74, doi: 10.1016/j.knosys.2013.10.010

[16] J. W. a. X. Lu, "Sustainable and Resilient Distribution Systems With Networked Microgrids [Point of View]," *Proceedings of the IEEE*, vol. 108, pp. 238-241, doi: 10.1109/JPROC.2019.2963605

[17] H. Oliveira, L. H. S. Santos, J. G. De Matos, L. A. d. S. Ribeiro, A. C. Oliveira and J. V. M. Caracas, "Challenges in Medium Voltage Microgrids Case Study: Alcântara Launch Center," in *IEEE 8th Southern Power Electronics Conference and 17th Brazilian Power Electronics Conference (SPEC/COBEP)*, Florianopolis, Brazil, 2023, doi: 10.1109/SPEC56436.2023.10408472

[18] C. A. S. e. a. Castelo Branco, "Mission Critical Microgrids: The Case of the Alcântara Space Center," *Energies*, vol. 15, p. 3226, 2022, doi: 10.3390/en15093226

[19] International Electrotechnical Commission (IEC). International Standard 186., *Voltage transformers*, 1987.

[20] Arcol, "https://www.ohmite.com/assets/docs/acl_ap101.pdf," Arcol. [Online]. [Accessed 8 11 2023].

[21] American National Standards Institute (ANSI), *IEEE Standard for Electrical Power System Device Function Numbers, Acronyms, and Contact Designations. C37.2.*, New York: IEEE, 2008.

[22] IEEE STANDARDS ASSOCIATION, IEEE Standard for Interconnection and Interoperability of Distributed Energy Resources with Associated Electric Power Systems Interfaces. IEEE Std 1547-2018, New York: IEEE, 2018.

[23] G. Kindermann, Proteção de Sistemas Elétricos de Potêncnia, Florianópolis: Ed. do Autor, 1999.

BIOGRAPHIES

Hércules Araújo Oliveira graduated with a bachelor's degree in mechanical engineering from the State University of Maranhão in 2015, Brazil. In the following years, he developed research in the field of automation and control, focusing on power converters, microgrids, and renewable energy sources. In 2017, he received a master's degree in electrical engineering from the Federal University of Maranhão, Brazil. In 2018, he started working on research in the area of ocean energies as a PhD student member of the Brazilian National Institute of Science & Technology of Ocean Energy. In 2019, he was a Graduate Visiting Student at the Schulich School of Engineering at the University of Calgary, Canada, developing research to identify and analyze factors that influence the efficiency of a tidal and wind power plant. In 2023, he received a PhD degree in electrical engineering from the Federal University of Maranhão, Brazil. Currently, he is a postdoctoral student at the Energy Institute of the Federal University of Maranhão and Research and Innovation Coordinator at the Equatorial Group Institute of Science and Technology.

Luiza Higino Silva Santos graduated in Electrical Engineering from the Pontifical Catholic University of Campinas in 2019. During undergraduate studies, participated in four Scientific/Technological Initiation projects, one in the area of current sensors, two in the area of Renewable Energies, and one in Long-Range Wireless Technology (LoRa), all within the Energy Efficiency Research Group. In the master's degree program, in the Department of Systems and Energy of the State University of Campinas, conducted studies on modeling and simulation of microgrids. Currently, she is a doctoral student in the Department of Systems and Energy at the State University of Campinas, participant in the R&D project Microgrids for efficient, reliable and greener energy (MERGE), and member of the Paulista Center for Energy Transition Studies.

Luiz Antonio de S. Ribeiro (M'98) received the M.Sc. and Ph.D. degrees from the Federal University of Paraiba, Campina Grande, Brazil, in 1995 and 1998, respectively. During the period 1996–1998 and 2004–2006, he was a Visiting Scholar and Post doctor with the University of Wisconsin, Madison, WI, USA, working on parameter estimation and sensorless control of AC machines. In 2015, he was a Research Guest at Aalborg University, Denmark, working on power converters control for microgrid applications. He is currently a Full Professor with the Department of Electrical Engineering, Federal University of Maranhão, Brazil. His research interests include design and control of power electronics converters, microgrids, and renewable energy. Dr. Ribeiro received two IEEE Energy Conversion Congress and Exposition prize paper awards.

José Gomes de Matos was born in Brazil in 1957. He received the B.S. and M.S. degrees in electrical engineering from the Federal University of Campina Grande, Paraiba, Brazil, in 1980 and 1986, respectively, and the Ph.D. degree in electrical engineering from the Federal University of Maranhão, São Luís, Brazil, in 2014. Since 1980, he has been a Professor in the Electrical Engineering Department of the Federal University of Maranhão. His research interests include microgrids, control systems, power electronics, and power generation systems based on renewable energy, particularly wind and photovoltaic sources.

Lucas de Paula Assunção Pinheiro received the M.Sc. in Energy and Environment from the Federal University of Maranhão, Brazil in 2019. He worked at Equatorial Energia, managing Research and Development (R&D) and Energy Efficiency (EE) projects. He coordinates Innovation Projects, managing development teams, monitoring delivery of products according to schedules and technically validating the products with the sponsors within electric energy distributors. Currently, he is an Executive at the Institute of Science and Technology Grupo Equatorial.